

Transport Analysis of RF Drift-velocity Filter Employing Crossed DC and AC Electric Fields for Ion Swarm Experiments*

K. Iinuma and M. Takebe

Department of Nuclear Engineering, Tohoku University,
Aramaki, Aobaku, Sendai, 980 Japan.

Abstract

The operational characteristics of the RF drift-velocity filter developed recently by us to separate a mixture of gaseous ions are examined theoretically. The solutions of the appropriate transport equations provide an analytical formula for the transmission efficiency of the filter in terms of the mobility and diffusion coefficient of the ions, the electric field strength, the RF frequency and the filter dimension. Using the experimental transport data for Li^+/Xe and Cs^+/Xe , the formula was tested and we find that it adequately accounts for the degree of ion separation achieved by the filter at high gas pressures. The variation of the profiles of the arrival time spectra for Li^+ , Na^+ and Cs^+ ions in CO_2 , obtained by our drift-tube experiments, also supports this analysis.

1. Introduction

In swarm experiments ion species may quickly change their identity through reactions. The most popular method of identifying the ion species is by the use of a mass spectrometer. However, the mass spectrometer cannot operate at high gas pressures and it is the usual procedure to adopt differential pumping to separate the ions from the gas. Differential pumping has some problems: a sampling section may accelerate ion reactions and an ion species present at high gas pressure may change its identity in the differentially pumped section; the transmission efficiency may vary with the ion species and thus cause mass-discrimination effects. Recently, we have developed an RF drift-velocity filter which operates at high gas pressures (Iinuma *et al.* 1995) in order to avoid these problems.

The idea of an ion filter was proposed and tested by Eiber (1963). He aimed to separate ion species with a filter consisting of a set of wires with spacing less than a mean free path. Our filter, however, has a much larger distance between foils and separates a mixture of ions, at a gas pressure of about 1 Torr ($\equiv 133$ Pa), according to their different mobilities. Although we confirmed its success in ion swarm experiments, a theoretical analysis has been lacking. This paper deals with a model analysis to examine the characteristics of the filter employing crossed electric fields, and in particular the derivation and numerical testing of its transmission efficiency as a function of the frequency of the AC field.

* Refereed paper based on a presentation to the Third Japan–Australia Workshop on Gaseous Electronics and Its Applications, held at Yeppoon, Queensland, in July 1994.

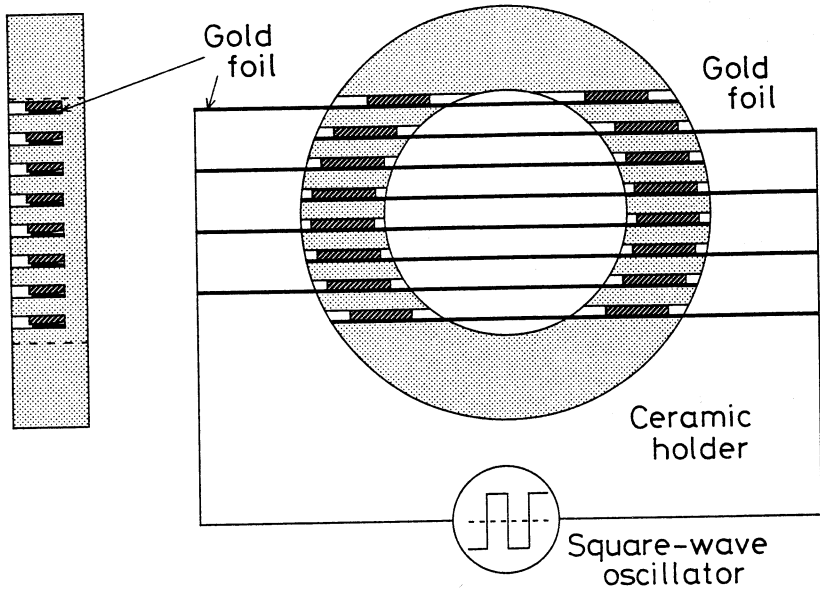


Fig. 1. Illustration of the RF drift-velocity filter. The material shown by diagonal lines is insulation to hold the gold foil in position.

2. RF Drift-velocity Filter

The drift-velocity filter consists of eight gold foils, 0.05 mm thick, 2.0 mm wide, placed in parallel 2.0 mm apart on a ceramic holder. A schematic view of the filter is shown in Fig. 1. The filter operates in the following way: E_x is the main DC drift field in which ions drift with velocity v_x , while E_y is a periodic AC field perpendicular to E_x in which the ions oscillate between the foils with drift velocity v_y . For a given AC frequency an ionic species with a sufficiently large value of v_y will be collected by a foil and cannot pass through, whereas an ion with a smaller value of v_y will not be captured and can transmit through the filter.

3. Simplified Kinetic Model of the Filter

In the present analysis E_y is assumed to be produced by a square-wave AC potential of frequency f . We first use a simplified kinetic model to derive an approximate expression for the transmission efficiency ξ_A as a function of f ; this will be compared with a more sophisticated expression ξ . Let us assume that all the ions transverse the gap length between the foils, $2a$, with the same velocity v_y during the half-period $1/2f$. So, the following inequality needs to be satisfied in order for all ions to be trapped:

$$v_y \geq 4af. \quad (1)$$

If f is varied complete trapping of the ions occurs at $f = f_c$ given by

$$v_y = 4af_c, \quad (2)$$

where f_c is the corresponding frequency of the AC field. Since the reduced mobility K_0 is related to the drift velocity v_{dr} (cm s^{-1}) by

$$K_0 = 3.7215 \times 10^{-3} \frac{v_{dr}}{E/N} \text{ cm}^2 \text{ V}^{-1} \text{ s}^{-1}, \quad (3)$$

where E is the electric field strength and N the gas number density (E/N is in Td), we have the substitution

$$f_c = 67.2 \frac{K_0 E_y/N}{a} \text{ Hz}, \quad (4)$$

with a in cm. We define the transmission efficiency ξ_A as

$$\xi_A = 1 - f_c/f, \text{ for all } f \geq f_c. \quad (5)$$

In the limit $f \rightarrow \infty$ all the ions can pass through the filter and $\xi_A = 1$.

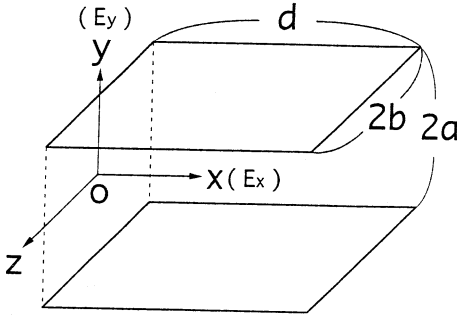


Fig. 2. Cartesian coordinate system for analysing the behaviour of an ion swarm in crossed electric fields. The main DC field E_x and the AC periodic field E_y are applied along the x and y axes respectively, while there is no electric field in the z direction. Thermal diffusion therefore dominates the ionic motion in the z direction.

4. Transport Analysis of the Filter

The expression (5) is useful as it stands, yielding a reasonable approximation to the ξ - f curve. This model, however, ignores two inevitable effects which may change the ξ - f curve unfavourably. These are nonuniformity of the E_x and E_y fields and diffusion of ions occurring in the filter. We now develop a more realistic model by taking these effects into account.

The distortion of the E_x and E_y fields arises in the vicinity of the filter, where the transport phenomena of the ions become inhomogeneous or position dependent. While the numerical analysis in such a case is not meaningless for designing a real filter, no information on the relation between the factors governing ξ can be obtained analytically. In addition, we usually set the E_y field to be much larger than the E_x field in our experiment ($E_y/N \gg E_x/N$). We therefore assume that the distortion of the E_y field becomes small enough to be neglected. Under this condition it is possible to derive an analytical formula for ξ which strongly depends on diffusion at low gas pressures. A solution of the transport equation with appropriate initial and boundary conditions is used for this aim.

To this end we define the Cartesian coordinate system shown in Fig. 2, with the E_x and E_y fields being directed along the x and y axes respectively. No electric

field is applied along the z axis perpendicular to the x - y plane. The motion of the ions along the x , y and z axes is assumed to be entirely independent. The number density of ions $N(r, t)$ can be represented by the product of three line densities, $X(x, t)$, $Y(y, t)$ and $Z(z, t)$:

$$N(r, t) = X(x, t) Y(y, t) Z(z, t). \quad (6)$$

The spatio-temporal behaviour of an ion swarm in the filter is governed by the following three transport equations:

$$\frac{\partial X}{\partial t} = D_x \frac{\partial^2 X}{\partial x^2} = v_x \frac{\partial X}{\partial x}, \quad (7)$$

$$\frac{\partial Y}{\partial t} = D_y \frac{\partial^2 Y}{\partial y^2} + (-1)^k v_y \frac{\partial Y}{\partial y}, \quad (8)$$

$$\frac{\partial Z}{\partial t} = D_z \frac{\partial^2 Z}{\partial z^2}. \quad (9)$$

Here D_x , D_y and D_z are the components of the diffusion coefficient in the x , y and z directions respectively. The integer k in (8) denotes the number of half-cycles of the AC electric field, in each of which the direction of drift motion along the y axis is alternately changed.

We now introduce the following initial boundary conditions:

$$X(x, 0) = \delta(x), \quad (10)$$

$$Y(y, 0) = H(y + a) - H(y - a), \quad (11)$$

$$Z(z, 0) = H(z + b) - H(z - b), \quad (12)$$

$$Y(\pm a, t) = 0, \quad (13)$$

$$Z(\pm b, t) = 0, \quad (14)$$

where $\delta(x)$ and $H(y)$ are the delta function and Heaviside step function respectively. Making use of these conditions and defining $1/2f$ as τ , we derive the solutions of (7), (8) and (9) as

$$X(x, t) = \frac{1}{(4\pi D_x t)^{1/2}} \exp\left(-\frac{(x - v_x t)^2}{4D_x t}\right), \quad (15)$$

$$Y(y, k\tau) = \frac{1}{(4\pi D_y \tau)^{1/2}} \int_{-a}^a f_{k-1}(\zeta) \exp\left(-\frac{[\zeta - y - (-1)^k v_y \tau]^2}{4D_y \tau}\right) d\zeta, \quad (16)$$

where $f_{k-1}(y)$, expressed by

$$f_{k-1}(y) = [H(y+a) - H(y-a)]Y(y, (k-1)\tau), \quad (17)$$

is the spatial distribution of ions at $(k-1)\tau$ which governs its drift and diffusive motion during the period of time $(k-1)\tau \leq t \leq k\tau$. The function $Z(z, t)$ is also represented by an integral,

$$Z(z, t) = \frac{1}{\pi^{1/2}} \int_{\eta'}^{\eta} \exp(-\beta^2) d\beta. \quad (18)$$

Here η and η' are denoted by

$$\eta = (z+b)/(4D_z t)^{1/2}, \quad \eta' = (z-b)/(4D_z 4t)^{1/2}. \quad (19)$$

Solution (15) as well as (18) describes a typical near-Gaussian profile, whereas (16) displays the stepwise behaviour of the line density in the region $-a \leq y \leq a$ at $k\tau$ ($k = 1, 2, 3, \dots$).

The transmission efficiency ξ , including the effect of diffusion, is defined as

$$\xi = \frac{1}{4ab} \int_{-a}^a \int_{-b}^b Y(y, k\tau) Z(z, \tau_0) dy dz, \quad (20)$$

where the mean transit time is

$$\tau_0 = d/v_x, \quad (21)$$

d is the drift length along the x axis (see Fig. 2), and the relation $\tau_0 = k/2f$ is to be satisfied.

5. Results and Discussion

Our primary interest is to calculate the number density of ions moving periodically between the foils. A simple quadrature is applied to carry out the numerical integration of (16). All the transport coefficients required are taken from the experimental data compiled by Ellis *et al.* (1978, 1984). The resulting number density $Y(y, k\tau)$ for Li^+ ions in Xe is displayed in Figs 3, 4 and 5 for three different values of the diffusion coefficient. Their motion is limited to the region $-0.5 \leq y \leq 0.5$ cm. For this calculation, τ , f and k are set at $4.34 \mu\text{s}$, 115.1 kHz and 32 respectively.

In the case where a small diffusion coefficient is used (see Fig. 3), the percentage of surviving ions is mainly dominated by the drift velocity, and is not seriously affected by diffusion. The larger the value of D_y , the more the diffusion process becomes important (see Fig. 4). Finally, most of the ions will be trapped and absorbed on the foils due to diffusion, and are not able to pass through the filter (see Fig. 5).

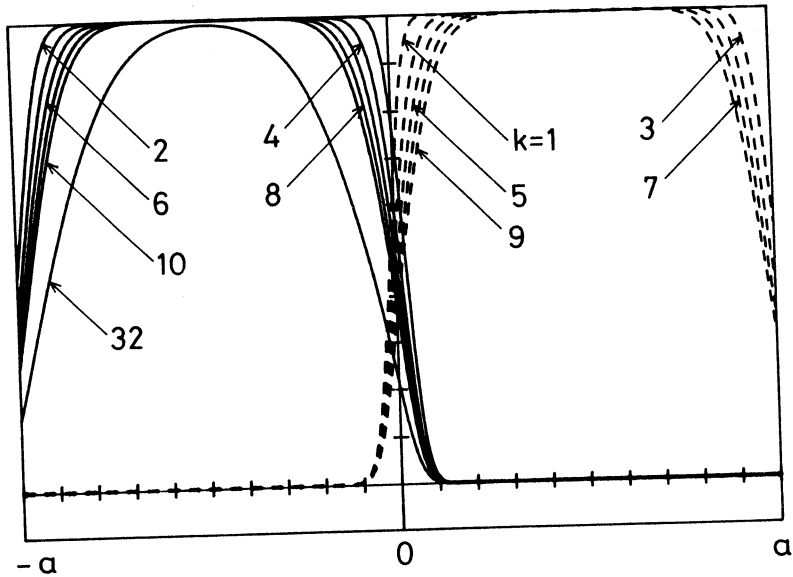


Fig. 3. Line density $Y(y, k\tau)$ of Li^+ ions in Xe along the y axis with a small value of D_y . The calculation of $Y(y, k\tau)$ in the range $-0.5 \leq y \leq 0.5$ cm ($a = 0.5$ cm) is repeated 32 times: $v_x = 7.2 \times 10^3$ cm s $^{-1}$, $v_y = 1.13 \times 10^5$ cm s $^{-1}$, $D_y = 33.5$ cm 2 s $^{-1}$, $d = 1$ cm, $f = 115.1$ kHz, $\tau = 4.34$ μ s and $\tau_0 = 139$ μ s. The initial condition is $Y(y, 0) = H(y + 0.5) - H(y - 0.5)$. The dashed curves depict $Y(y, k\tau)$ for Li^+ ions drifting and diffusing from left to right, whereas the solid curves are those moving from right to left. The density $Y(y, (k-1)\tau)$ is employed for the initial condition to calculate $Y(y, k\tau)$. Only the ions shown by the last profile $Y(y, 32\tau)$, which arrive at the end of the filter along the x axis, can pass through the filter; the percentage of surviving ions is 38.5%.

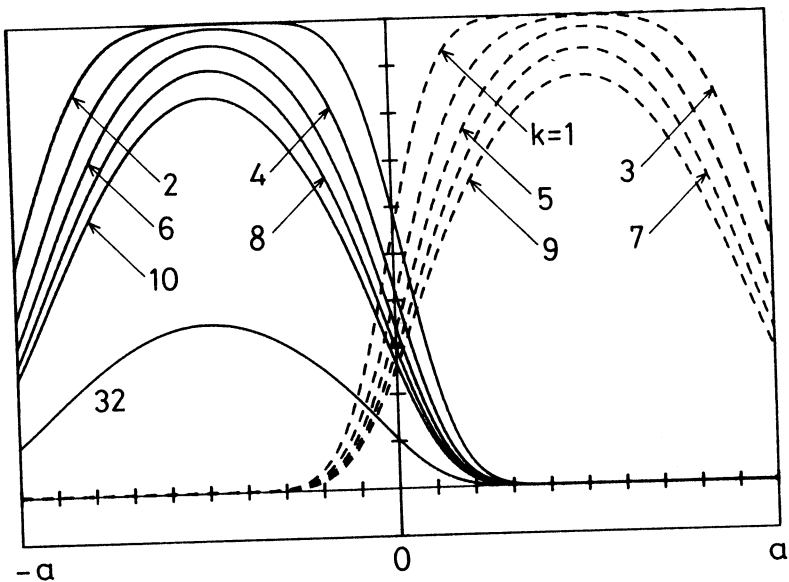


Fig. 4. The same as for Fig. 3, except for a D_y value of 335 cm 2 s $^{-1}$. The percentage of surviving ions is 13.6%.

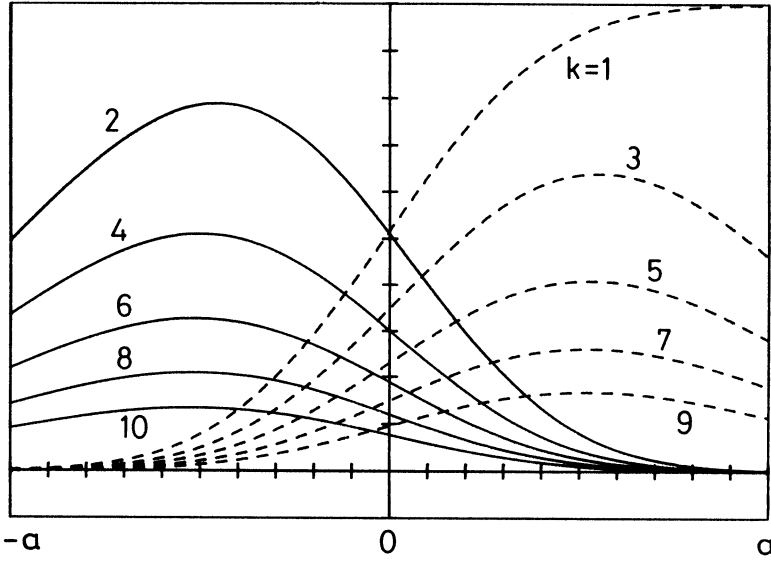


Fig. 5. The same as for Fig. 3, except for a D_y value of $3350 \text{ cm}^2 \text{ s}^{-1}$. Note that in this case most of the Li^+ ions in the filter are trapped and absorbed because of the extremely large diffusion coefficient; the percentage of surviving ions is only $4.7 \times 10^{-2}\%$, where profile number 32 and the horizontal axis now entirely overlap.

Next, making use of expression (20), we obtain the ξ - f curves for the Li^+/Xe and Cs^+/Xe systems and examine their difference in order to provide information for designing the filter. For both systems, an E_x/N of 10 Td and E_y/N of 100 Td are employed ($1 \text{ Td} \equiv 10^{-17} \text{ V cm}^2$). These results are depicted in Figs 6 and 7 respectively, along with ξ_A for the sake of comparison. A marked difference between the two systems is that of the frequency at which the curves start to rise. The frequency for the Li^+/Xe system is about 40 kHz, while that for the Cs^+/Xe system is about 7 kHz: the corresponding values of f_c calculated from (4) are 56.5 and 12.9 kHz respectively. This difference indicates that a separation of Li^+ and Cs^+ ions is possible. Namely, when we fix the RF frequency somewhere between 7 and 40 kHz, a fraction of the Cs^+ ions can pass through the filter, whereas most of the Li^+ ions are trapped. One more feature of these figures is the effect of diffusion on the transmission efficiency. As the diffusion coefficient becomes much larger, so the ξ - f curve becomes flatter, showing that the percentage of transmitted ions decreases. Extremely large diffusion may, therefore, render the RF filter ineffective.

Finally we show three sets of arrival time spectra (ATS) in Figs 8, 9 and 10, obtained experimentally with/without the filter mounted on our drift-tube apparatus. The apparatus and the measurement system have been reported previously in detail (Iinuma *et al.* 1995). These ATS indicate that the above analysis is appropriate and that the present idea is basically correct, although the resolution of the filter is still extremely low mainly because of the low gas pressure adopted in the present experiments. Fig. 8 shows two sets of ATS for the Li^+/CO_2 system, obtained by varying the pulse height, V_{RF} (or E_y), of the square wave. The peak on the left is the ATS of unclustered Li^+ ions which

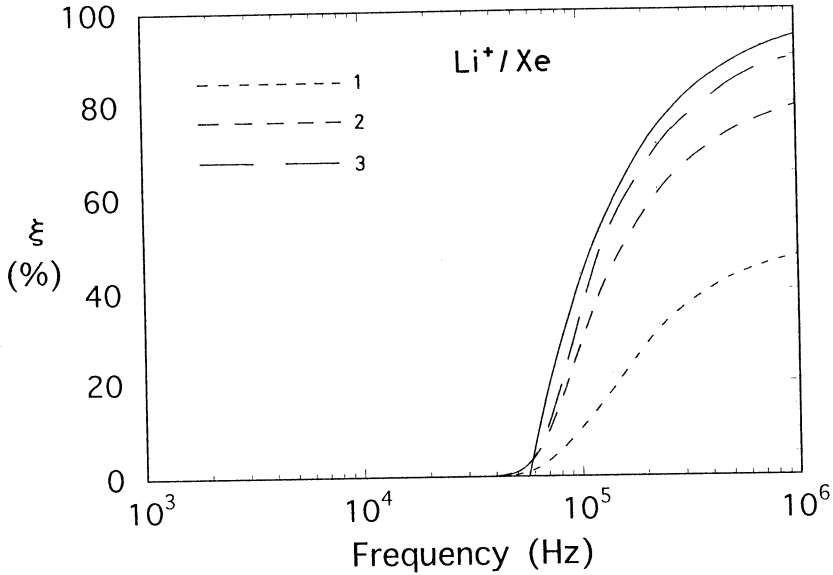


Fig. 6. Theoretical transmission efficiency of the filter for Li^+ ions in Xe plotted versus the RF frequency. The transport coefficients used in the calculations are the same as those employed in Fig. 3. Curves 1, 2 and 3 are those calculated from equation (20), using D_y values of 335, 33.5 and $3.35 \text{ cm}^2 \text{ s}^{-1}$ respectively. The thermal value of D_z is also employed in this analysis. The solid curve is obtained from equation (5) with $f_c = 56.5 \text{ kHz}$, $a = b = 0.5 \text{ cm}$ and $d = 1 \text{ cm}$.

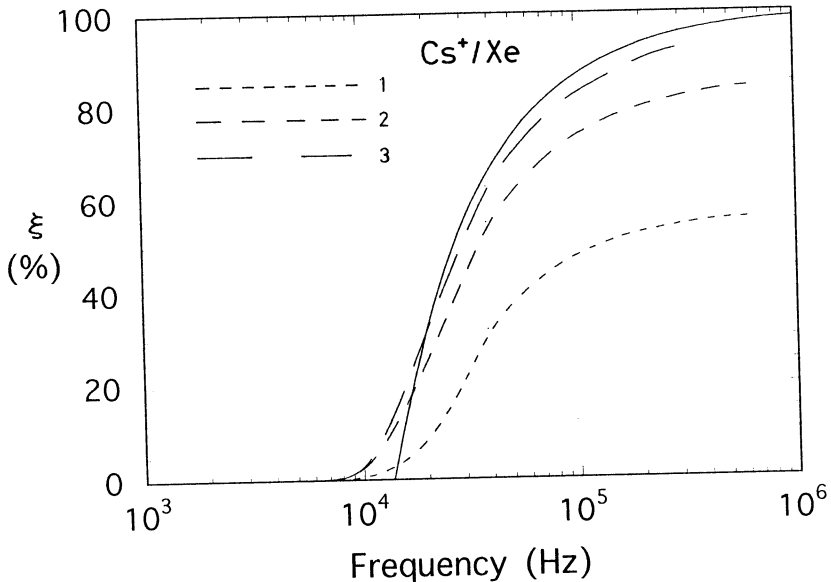


Fig. 7. The same as for Fig. 6, for Cs^+ ions in Xe. Curves 1, 2 and 3 are those obtained using D_y values of 68.9, 6.89 and $0.689 \text{ cm}^2 \text{ s}^{-1}$ respectively. The value of f_c for the solid curve is 12.9 kHz, while $V_x = 2.4 \times 10^3 \text{ cm s}^{-1}$, $V_y = 2.58 \times 10^4 \text{ cm s}^{-1}$ and $\tau_0 = 416.7 \mu\text{s}$.

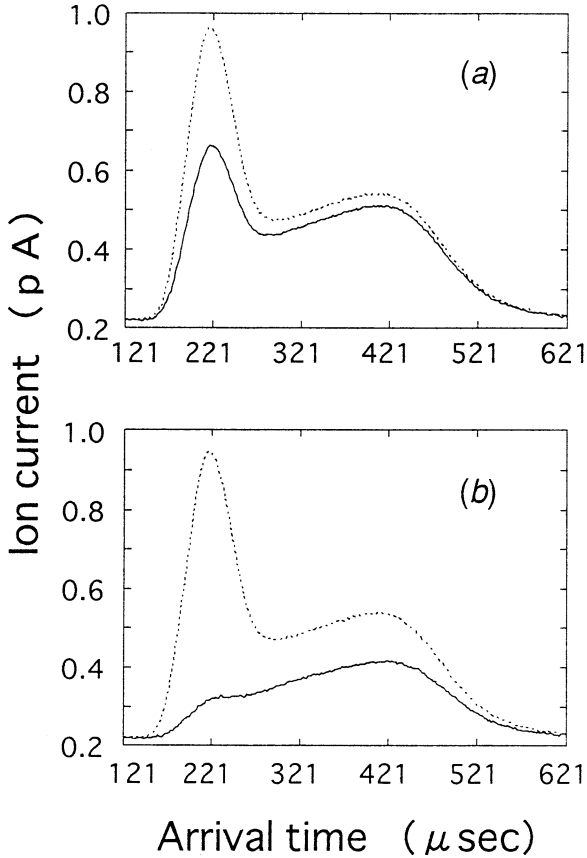


Fig. 8. The V_{RF} (or E_y) dependence of an ATS for the Li^+/CO_2 system: (a) $V_{\text{RF}} = \pm 2$ V and (b) $V_{\text{RF}} = \pm 4$ V. The dotted ATS are obtained without operating the filter, while the solid ATS are obtained with it. The experimental conditions are $p = 0.2$ Torr, $T = 294$ K, $E_x = 4$ V cm^{-1} , $E_x/N = 60.9$ Td, $f = 1$ MHz and the drift distance is 8 cm.

produce Li^+CO_2 cluster ions by ion/molecule reactions, the ATS of which is shown as a ramped-shape profile on the right. We find that when E/N becomes large, the ions having larger mobility will be trapped more efficiently (see Fig. 8b). For the same combination three sets of ATS are obtained by varying the frequency f , as shown in Fig. 9. The lower the frequency, the smaller the fraction of Li^+ ions passing through the filter. These experimental facts are explained by formulas (4) and (5). Fig. 10 displays two ATS for a mixture of Li^+ , Na^+ and Cs^+ ions in CO_2 . The dot-dash curve is the ATS measured without operating the filter, while the solid curve is measured with it. It is apparent that a large fraction of the Li^+ ions, compared to Na^+ and Cs^+ ions, is trapped when the filter operates.

The analysis and the experimental results described above give us some clues for increasing the resolution of the present filter; first, operation at high gas pressure is essential, according to Figs 3, 4 and 5. Secondly, expression (5) shows that the slope of the curve at $f = f_c$ should be chosen as large as possible.

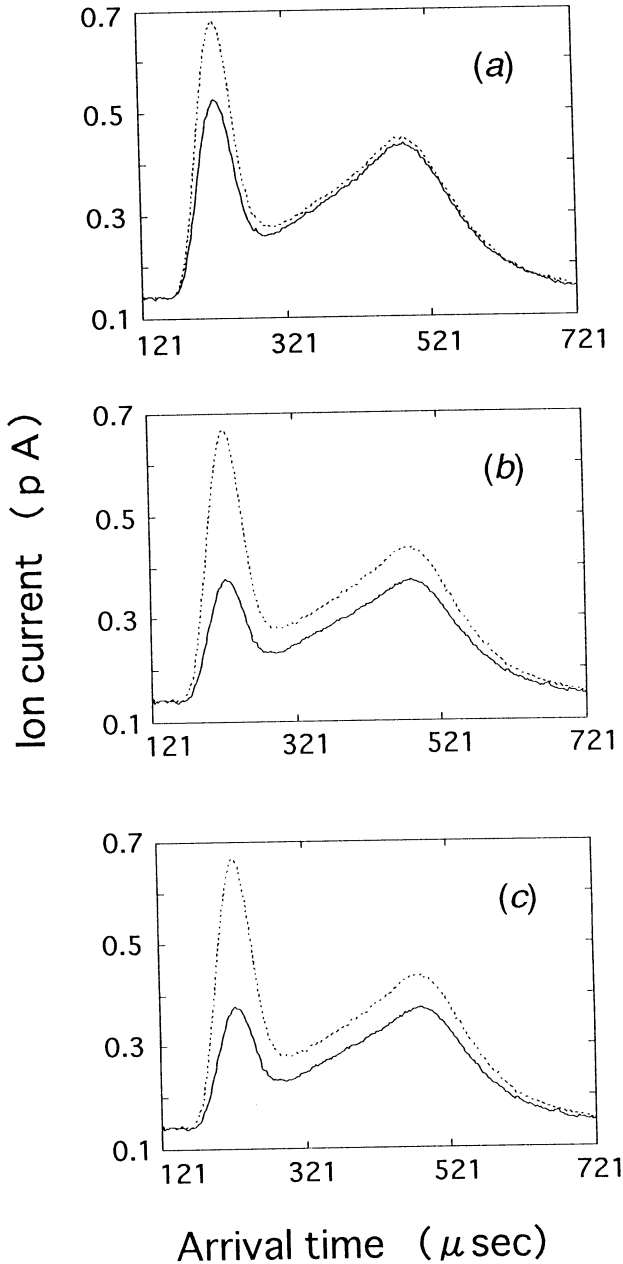


Fig. 9. RF frequency dependence of the ATS for the Li^+/CO_2 system: (a) $f = 2$ MHz, (b) $f = 750$ kHz and (c) $f = 200$ kHz. The dotted ATS are obtained without operating the filter, while the solid ATS are obtained with it. The experimental conditions are: $p = 0.25$ Torr, $T = 293$ K, $E_x = 5$ V cm^{-1} , $E_x/N = 60.7$ Td, $V_{\text{RF}} = \pm 2.5$ V and the drift distance is 8 cm.

Therefore, smaller values of f_c for both ion species may be favourable because the slope is equal to f_c^{-1} . This requires the use of a large value of a as well as a small value of $K_0 E_y/N$, followed by the expression (4). Thirdly, we note that

the use of too large a value of a will decrease the difference between the two cutoff frequencies $|f_{c1} - f_{c2}|$, and this makes it difficult to fix the frequency of operation at a value between them. Thus, an appropriate choice of parameters is needed for the RF filter to operate with much higher resolution.

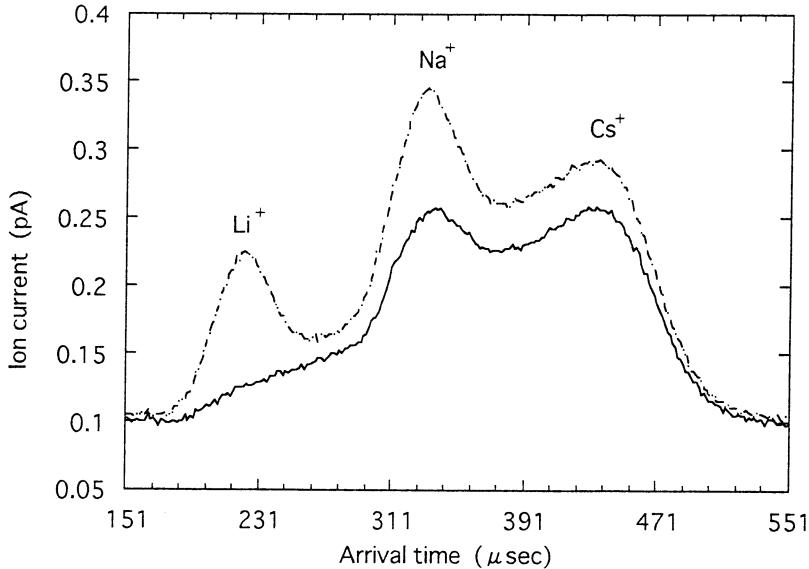


Fig. 10. Two ATS for a mixture of Li^+ , Na^+ and Cs^+ ions in CO_2 ; the dot-dash ATS is obtained without operating the filter, while the solid ATS is obtained with it. The experimental conditions are $p = 0.298$ Torr, $T = 296$ K, $E_x = 6$ V cm^{-1} , $E_x/N = 60.9$ Td, $V_{\text{RF}} = \pm 3$ V, $f = 2.4$ MHz and the drift distance is 8 cm.

6. Conclusions

A theory, based upon both a simplified kinetic model and a more elaborated transport analysis, has been developed to analyse the performance of an RF drift-velocity filter for separating a mixture of ions in gases. The analysis has been applied to the Li^+/Xe and Cs^+/Xe systems and has proved to be useful. Some experimental arrival time spectra for $(\text{Li}^+, \text{Na}^+, \text{Cs}^+)/\text{CO}_2$ combinations obtained by a drift-tube apparatus are demonstrated, which give positive support to the theoretical results.

Acknowledgments

The authors wish to thank T. Takahashi, T. Hamano, T. Ohtomo, K. Furukawa, Y. Satoh and T. Koike for their help in carrying out the experiment and for preparing this article. Also, T. Takahashi, K. Komatsu, T. Nagaya, M. Fujisawa and C. Akama are acknowledged for their assistance in the construction of the experimental setup. This work is supported by a Grant-in-Aid for Scientific Research from the Ministry of Education, Science and Culture of Japan.

References

- Eiber, H. (1963). *Z. Angew. Phys.* **15**, 461.
- Ellis, H. W., McDaniel, E. W., Albritton, D. L., Viehland, L. A., Lin, S. L., and Mason, E. A. (1978). *At. Data Nucl. Data Tables* **22**, 179.
- Ellis, H. W., Thackston, M. G., McDaniel, E. W., and Mason, E. A. (1984). *At. Data Nucl. Data Tables* **31**, 113.
- Iinuma, K., Takahashi, T., Kawanishi, T., Hamano, T., Ohtomo, T., Satoh, Y., and Takebe, M. (1995). *Int. Mass Spectrom. Ion Processes* (in press).

Manuscript received 5 December 1994, accepted 24 March 1995